Simulated flux-lattice melting and magnetic-field distributions in high-T_c superconductors

J.W. Schneider, S. Schafroth, and P.F. Meier
Physik-Institut der Universität Zürich, CH-8057 Zürich, Switzerland
(Received 9 February 1995)

Numerical calculations of the magnetic-field distribution $p(B)$ in high-T_c superconductors have been performed for different regimes of the B-T phase diagram to provide a basis for the interpretation of results from muon spin rotation experiments, which measure $p(B)$ directly. Using a Monte Carlo approach, flux-lattice melting was simulated and the corresponding $p(B)$ was obtained. Both above and below the melting transition, we find excellent agreement with the line shapes measured in a recent experiment in $Bi_2Sr_2CaCu_2O_8$ if in addition the shape of the sample is taken into account.

I. INTRODUCTION

Highly anisotropic or layered high-T_c superconductors such as the Bi-based compounds may show a variety of flux-line structures in a magnetic field applied along the c axis.[1] For example at low temperatures and small fields we expect a nearly ideal Abrikosov flux-line lattice composed of London vortices. At higher fields or temperatures both pinning-caused static disorder and thermal fluctuations of the highly flexible vortex cores become possible.[1] In these phases the vortex cores threading the superconducting layers may be thought of as wiggly lines that are more appropriately described by chains of vortex dots or "pancakes."[2] In the past, computer simulations of vortex lattice melting based on various models[3–5] have shed some light on the essentials of the problem. However, the exact nature of the phase diagram is still far from being understood.

The magnetic-field distribution $p(B)$ in superconductors can be obtained directly from muon spin rotation (μSR) experiments. Positive muons are stopped in the sample at sites which are random with respect to the ideal or distorted flux-line lattice. Their precession in the local magnetic field is monitored via the decay positrons. The resulting time-dependent muon polarization $p_\mu(t)$ is then Fourier transformed to yield $p(B)$.[6]

It has been shown theoretically that the width σ of $p(B)$ is highly sensitive to the type of disorder.[7] For example randomly positioned stiff parallel flux lines tend to *increase* σ, whereas vortex-dot fluctuations may *decrease* σ. However, until now a direct comparison between theory and experiment was not possible since existing theories usually do not give the full line shape explicitly.[8] The situation is made worse by the fact that a comparison of the measured and the theoretical width is often meaningless, e.g., for highly asymmetric line shapes where the experimental σ is systematically underestimated and in addition depends on statistics.[10] The absence of theoretical line shapes is especially unfortunate since in a recent μSR experiment on high-quality single-crystal $Bi_{2.15}Sr_{1.85}CaCu_2O_{8+\delta}$ (BSCCO) the B-T plane has been sampled extensively using $p(B)$ as a probe.[11] The authors defined a dimensionless parameter

$$\alpha = M_3^{1/3}/M_2^{1/2} \tag{1}$$

to describe the asymmetry of the measured line shape, where M_2 and M_3 are the second and third moments of $p(B)$, respectively. In a first experiment, α was measured as a function of temperature at a fixed applied field $B_{\rm ext} = 45$ mT. An abrupt change of the line shape at about $T_m = 57$ K, i.e., well below the critical temperature ($T_c = 84$ K) where α dropped sharply from positive to negative values, was attributed to flux-lattice melting. In a second experiment, α was measured as a function of applied field at a fixed temperature of 5 K. The observation of a crossover field B_{2D} near 60 mT, above which α was reduced to about one-half of the low-field value, was interpreted in terms of a transition from a three-dimensional (3D) to a two-dimensional (2D) phase.[11]

This paper reports on results of numerical simulations of the full magnetic-field distribution $p(B)$ which was calculated for clusters of pancakes arranged specifically to represent the different regions of the B-T phase diagram. The flux-lattice melting was modeled following Ryu *et al.*[5] The Monte Carlo simulations reproduced their results for the temperature and field dependence of the hexatic order parameter and the mean-square deviation of the pancakes from their equilibrium sites. We determined the field distribution $p(B)$ by a spatial average of fields $\boldsymbol{B}(\boldsymbol{r})$ resulting from averaging $\boldsymbol{B}(\boldsymbol{r},t)$ over the thermal motion of the pancakes in equilibrium. In Sec. II the field of an individual pancake is considered in the London description. To check the cluster size dependence the field distribution is first calculated for a cluster where the pancakes in each 3D vortex line were aligned. Interactions between the pancakes are then introduced following Ref. 5. The resulting field distributions are discussed in Sec. III. It is shown that in order to compare the μSR data with the calculated $p(B)$ it is necessary to take the shape of the sample into account. The final Sec. IV is devoted to the conclusions.

II. MONTE CARLO SIMULATION OF INTERACTING PANCAKE VORTICES

It has been shown that 3D vortex lines can be built up by superposing the contributions of stacks of 2D pancake vortices.[2] Since the magnetic field $\boldsymbol{B}(\boldsymbol{r})$ is the vector sum of the contributions from all pancakes in the cluster, a given arrangement of pancakes completely determines $\boldsymbol{B}(\boldsymbol{r})$ and, as a consequence, the probability distribution $p(B)$ in the superconductor. The field of an individual pancake is cylindrically symmetric (with cylinder coordinates ρ, z) about a z axis parallel to the c axis of the crystal:[2]

$$b_z(\rho,z) = (\Phi_0/2\pi\Lambda r)\exp(-r/\lambda_{ab}) , \tag{2}$$

$$b_\rho(\rho,z) = (\Phi_0/2\pi\Lambda\rho)\,[\,(z/|z|) \times \exp(-|z|/\lambda_{ab}) - (z/r)\exp(-r/\lambda_{ab})\,] , \tag{3}$$

where $\Phi_0 = 2.0679 \times 10^{-15}$ T m^2 is the flux quantum, $\Lambda = 2\lambda_{ab}^2/s$ is the 2D thin-film screening length, λ_{ab} is the penetration depth in the ab planes, s is the stacking distance between the superconducting layers, and $r = (\rho^2+z^2)^{1/2}$. For the BSCCO sample used in the μSR experiments, appropriate values for λ_{ab} (at low temperatures) and s are[11] $\lambda_{ab} \approx 1800$ Å, $s \approx 15$ Å.

In a first step, such a calculation was performed for the case where the pancakes in each 3D vortex line were aligned and the flux lines formed an Abrikosov lattice with lattice constant $a_0 = (2\Phi_0/\sqrt{3}B)^{1/2}$. $p(B)$ was obtained as the histogram of the fields $B = |\boldsymbol{B}(\boldsymbol{r})|$ at typically 70×70 evenly spaced grid points in a unit cell of the magnetic lattice in a plane perpendicular to the z axis and at the center of the cluster ("unit cell"). The results were then compared to those from an exact numerical calculation[9] for different cluster sizes. As an example, an $8 \times 8 \times 160$ cluster (consisting of 160 layers of 8×8 pancakes) yielded a $p(B)$ where the second and third moments M_2 and M_3 agreed with the exact calculation to within 2%.

Two ideas led to the development of a Monte Carlo (MC) program to simulate flux-lattice melting: (1) The use of pancake-pancake interactions would lead to realistic clusters in thermal equilibrium at a given temperature, and (2) $p(B)$ could then be calculated from fields $\boldsymbol{B}(\boldsymbol{r})$ resulting from averaging $\boldsymbol{B}(\boldsymbol{r},t)$ over the thermal motion of the pancakes in equilibrium. The latter procedure would mimic the situation in a μSR experiment, where the relevant time scales for the muon (10^{-7}–10^{-6} s) are much greater than the typical correlation times for thermal motion of the pancakes (10^{-10} s).[12] As a starting point, a Monte Carlo program (MC1) was written using the approach described in Ref. 5. We employed the usual Metropolis algorithm on an $8 \times 8 \times 16$ cluster confined to a $256 \times 222 \times 16$ grid space. In a single MC step, each pancake makes a trial movement by one grid unit in plane z. Following Ryu *et al.*,[5] the following interactions were assumed to calculate the total cluster energy:

(A) Within plane z, all pancakes interact with each other according to

$$V_{ij}^z = T_0\,K_0\left(\frac{|\boldsymbol{r}_{i,z}-\boldsymbol{r}_{j,z}|}{\lambda_{ab}}\right) , \tag{4}$$

where $T_0 = \Phi_0^2 d/2\pi\lambda_{ab}^2\mu_0$, $d = 2.7$ Å is the thickness of the superconducting layers, $\mu_0 = 4\pi \times 10^{-7}$ V s A^{-1} m^{-1}, K_0 is the modified Bessel function of the second kind, $\lambda_{ab}(T) = \lambda_{ab}(0)[1-(T/T_c)^n]^{-1/2}$, and $n = 3.3$.[11] Within the planes, we used periodic boundary conditions, as did the authors of Ref. 5.

(B) Within line vortex i, a pancake interacts only with its two immediate neighbors above and below according to

$$V_i^{z,z+1} = \begin{cases} U_0\left[\frac{|\boldsymbol{r}_i^{z,z+1}|}{r_g} - 2\right] & \text{if } |\boldsymbol{r}_i^{z,z+1}| > 2\,r_g, \\ U_0\left[\frac{|\boldsymbol{r}_i^{z,z+1}|^2}{4r_g^2} - 1\right] & \text{otherwise,} \end{cases} \tag{5}$$

where $\boldsymbol{r}_i^{z,z+1} = \boldsymbol{r}_{i,z} - \boldsymbol{r}_{i,z+1}$, $r_g = \xi_{ab}/\sqrt{g}$, ξ_{ab} is the coherence length in the ab plane which has the same temperature dependence as λ_{ab} [$\xi_{ab}(0) \approx 15$ Å for BSCCO], g is a dimensionless interlayer coupling strength [$g = 1/2500$ for BSCCO (Ref. 5)], $U_0 = (T_0 a/\pi d)[1+\ln(\lambda_{ab}/a)]$, and $a = s - d = 12.3$ Å is the interlayer spacing. These interactions are obtained from the Lawrence-Doniach model of stacked superconducting layers[13] by approximating the full three-dimensional interaction with an effective two-dimensional interaction restricted to the same plane and the short-ranged Josephson interlayer coupling.

First, we used MC1 to find the thermal equilibrium of the cluster at $T = 10, 20, \ldots, 80$ K (starting with a triangular lattice at the lowest temperature). The total cluster energy was monitored as a function of the number of MC steps. Equilibrium was reached after typically 10^5 steps. In order to observe flux-lattice melting, we then calculated the hexatic order parameter Ψ_6 as well as the in-plane mean-square deviation $u_{\rm rms}$ of each pancake (i,z) from its average position $\boldsymbol{r}_{i,z}^{\rm ave} = \langle \boldsymbol{r}_{i,z}\rangle_{\rm MC}$ for these temperatures according to Ref. 5

$$\Psi_6 = \left\langle \frac{1}{Z_i}\sum_{j=1}^{Z_i} \exp[i6\theta_{ij}(\boldsymbol{r}_{i,z})] \right\rangle \tag{6}$$

and

$$u_{\rm rms} = \langle |\boldsymbol{r}_{i,z} - \boldsymbol{r}_{i,z}^{\rm ave}|^2\rangle^{1/2} . \tag{7}$$

Z_i is the coordination number for pancake (i,z), θ_{ij} is the bond angle for neighbors i and j with respect to a fixed direction, and the angular brackets indicate the average over all pancakes and over the MC steps. At low temperatures ($T < T_m$) and moderate fields ($B < B_{2D}$) where the pancakes form a nearly ideal Abrikosov lattice, Ψ_6 is expected to assume a value close to 1, whereas at temperatures above T_m, Ψ_6 should be close to zero. $u_{\rm rms}(T)$ should approximately follow

$$u_{\rm rms} = c\left[\frac{T/T_c}{(1-T/T_c)^{1/2}}\right]^{1/2} \tag{8}$$

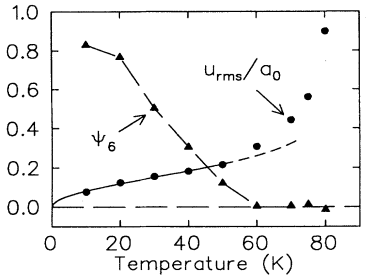

FIG. 1. The hexatic order parameter Ψ_6 (triangles) and the in-plane mean-square deviation $u_{\rm rms}$ of the pancakes from their average positions normalized by the magnetic lattice constant a_0 (circles) as calculated by MC1, with $B = 45$ mT. The solid curve is a fit of Eq. (8) to the calculated points in the regime 10–50 K and is expected to describe $u_{\rm rms}(T)$ *below* T_m. Note that both parameters indicate flux-lattice melting just below 60 K.

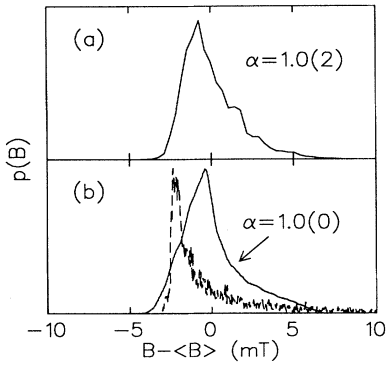

FIG. 2. (a) Measured magnetic-field distribution in BSCCO at $T = 6.6$ K and $B = 45$ mT (Ref. 14). (b) Dashed line: calculated curve using MC2 with $T = 10$ K and $B = 45$ mT, where $\Psi_6 \approx 1$ indicates the 3D line vortex phase. Solid line: calculated curve taking additionally into account the rectangular sample cross section.[17] $\langle B \rangle$ is the average field.

below T_m (see Houghton *et al.* in Ref. 1) and exhibit a sharp change of slope at T_m.[5] Figure 1 shows $\Psi_6(T)$ and $u_{\rm rms}(T)$ as calculated by MC1 over 3×10^4 MC steps at each temperature point in thermal equilibrium, with $B = 45$ mT. The solid curve is a fit to Eq. (8) in the regime 10–50 K, yielding $c = 518(1)$ Å. Note that both curves show the behavior expected for flux-lattice melting just below 60 K, in good agreement with the experimental observation[11] of an abrupt change of the line shape near $T_m = 57$ K.

III. MAGNETIC-FIELD DISTRIBUTIONS: RESULTS AND DISCUSSION

To calculate the magnetic-field distribution $p(B)$ the equilibrated clusters mentioned in Sec. II were used as building blocks to compose "superclusters" of $8 \times 8 \times 160$ pancakes in order to obtain meaningful field distributions. Test calculations showed that at least 100 planes of pancakes are needed to get realistic field distributions. A supercluster was obtained by first building an intermediate cluster with size $8 \times 8 \times 32$ consisting of the original cluster plus its mirror image (mirror plane $s/2$ above plane 16), and then stacking five such intermediate clusters on top of each other.

Subsequently, these superclusters were brought into thermal equilibrium using again MC1. The equilibrated superclusters were then used by a second program, MC2, to calculate the resulting field vectors at the grid points in the unit cell after every 50 MC steps, with a total of 10^4 steps. The thermally averaged field vectors were obtained as the average over all MC steps. Finally, $p(B)$ was calculated from the averaged field vectors. Note that if we associate the time interval between two consecutive MC steps with the correlation time for thermal motion of the pancakes (10^{-10} s),[12] the time interval over which the field vectors are averaged is just on the order of the muon lifetime (10^{-6} s), as in a μSR experiment.

Figure 2(b) (dashed curve) shows $p(B)$ calculated with MC2 for $B = 45$ mT and $T = 10$ K, i.e., *below* T_m. Note the distinct shape characteristic of a 3D flux structure, in particular the long tail at high fields arising from regions close to the vortex cores. The larger width of the measured curve [Fig. 2(a)] can be explained by taking into account the rectangular cross section of the flat, approximately circular crystals. In such samples the flux density near the sample edges will be lower than at the center following[15]

$$B(r) = B_{\rm ext} - \mu_0 m_{\rm eq} H_{c1}\{1 - [1 - (r/r_0)^2]^{1/2} + d_0/2r_0\}, \tag{9}$$

where $r = 0$ corresponds to the center of the sample with radius r_0 and thickness d_0 (for the BSCCO sample used in the experiment, $r_0 \approx 1.3$ mm and $d_0 \approx 0.5$ mm), $H_{c1} = \Phi_0 \ln(\kappa)/4\pi\mu_0\lambda_{ab}^2$ is the lower critical field, $\kappa = \lambda_{ab}/\xi_{ab}$, and $\mu_0 m_{\rm eq} H_{c1}$ is the equilibrium mag-

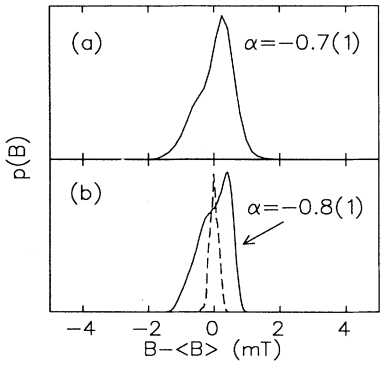

FIG. 3. (a) Measured magnetic-field distribution in BSCCO at $T = 64$ K and $B = 45$ mT (Ref. 14). (b) Dashed line: calculated curve using MC2 with $T = 80$ K and $B = 45$ mT, where $\Psi_6 \approx 0$ indicates the liquid phase. Solid line: calculated curve taking additionally into account the rectangular sample cross section.

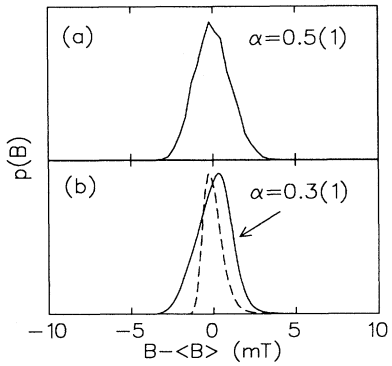

FIG. 4. (a) Measured magnetic-field distribution in BSCCO at $T = 5$ K and $B = 90$ mT (Ref. 14). (b) Dashed line: calculated curve using PAN3 with $B = 90$ mT with no correlation between the adjacent layers, but with an Abrikosov lattice in the planes, corresponding to a 2D phase. Solid line: calculated curve taking additionally into account the rectangular sample cross section (Ref. 17).

netization. The dimensionless quantity m_{eq} depends only weakly on field and temperature in the parameter range of relevance. It is given by[16]

$$m_{eq} = \ln(\beta' a_0/\xi)/\ln(\lambda/\xi), \tag{10}$$

with $\beta' = 0.231$. In all calculations a value of 0.5 has been assigned to m_{eq}.

This effect of the sample shape must not be neglected. It can be simulated by randomly shooting virtual muons onto a virtual sample. The hit position determines the field shift from the external field according to Eq. (9). The distribution $p(B)$ resulting from MC2 [Fig. 2(b), dashed curve] is then shifted by this amount. The process is repeated about 1000 times and the final $p(B)$ [Fig. 2(b), solid curve] is obtained as the average of the individual distributions. The agreement of the line shape, and consequently of the asymmetry α, with experiment [Fig. 2(a)] is now excellent.

Figure 3(b) (dashed curve) shows $p(B)$ calculated with MC2 for $B = 45$ mT and $T = 80$ K, i.e., *above* T_m. Note the complete disappearance of the high-field tail in the melted cluster due to averaging over the now substantial thermal motion of the pancakes. A comparison with experiment [Fig. 3(a)] shows that while the calculated curve is narrow and symmetric, the measured distribution is wider and exhibits a distinct low-field tail, giving rise to a negative α. All features of the measured curve, including the sign and magnitude of α, can again be explained by taking into account the true sample geometry [Fig. 3(b), solid curve].

To simulate 2D flux structures, where disorder induced by random pinning reduces the correlation between the pancake positions in adjacent layers, a $10 \times 10 \times 200$ cluster was taken where the individual planes were made up of vortex dots arranged in an Abrikosov lattice, but with the planes both shifted and rotated randomly with respect to one another (program PAN3). $p(B)$ was then calculated for $B = 90$ mT as the average over 500 such random clusters [Fig. 4(b), dashed curve]. Note the distinctly different shape of the field distribution, both with respect to that in Fig. 2 and in Fig. 3. As in Figs. 2(b) and 3(b), the final $p(B)$, which is shown in Fig. 4(b) (solid curve), was obtained by additionally accounting for the geometry effect [Eq. (9)]. Again, the calculated line shape agrees well with the measurement [Fig. 4(a)].

IV. CONCLUSIONS

In conclusion, we have performed numerical calculations of the magnetic-field distribution in the mixed state of an anisotropic high-T_c superconductor in three different regimes of the B-T phase diagram, i.e., in the 3D line vortex phase (Fig. 2), in the liquid phase (Fig. 3), and in the 2D phase (Fig. 4). We find that each phase gives rise to a distinct *shape* of the field distribution. Our line shapes, which have been calculated using the appropriate parameters for BSCCO, but no adjustable parameters, are in excellent agreement with those obtained in a recent μSR experiment on this superconductor. The measured curves in the 3D and the liquid phases can be explained by averaging the field vectors in the model sample over the thermal motion of the pancakes and by taking into account the rectangular sample cross section. Our calculations, which can easily be adapted to other anisotropic high-T_c superconductors, thus provide a firm basis for the interpretation of experimentally obtained magnetic-field distributions in these materials.

ACKNOWLEDGMENTS

We thank H. Keller and S.L. Lee for many helpful and stimulating discussions and N. Paschedag for assistance with the computing environment. This work was supported by the Swiss National Science Foundation (NFP30 Grant No. 4030-32785).

[1] See, e.g., A. Houghton, R.A. Pelcovits, and A. Sudbø, Phys. Rev. B **40**, 6763 (1989); D.S. Fisher, M.P.A. Fisher, and D.A. Huse, *ibid.* **43**, 130 (1991); L.I. Glazman and A.E. Koshelev, *ibid.* **43**, 2835 (1991).
[2] J.R. Clem, Phys. Rev. B **43**, 7837 (1991).
[3] L. Xing and Z. Tešanović, Phys. Rev. Lett. **65**, 794 (1990).
[4] Y.-H. Li and S. Teitel, Phys. Rev. Lett. **66**, 3301 (1991).
[5] S. Ryu, S. Doniach, G. Deutscher, and A. Kapitulnik, Phys. Rev. Lett. **68**, 710 (1992).
[6] See, e.g., B. Pümpin *et al.*, Phys. Rev. B **42**, 8019 (1990).
[7] E.H. Brandt, Phys. Rev. Lett. **66**, 3213 (1991).
[8] $p(B)$ for an Abrikosov lattice is given, e.g., in Ref. 9.
[9] S.L. Thiemann, Z. Radović, and V.G. Kogan, Phys. Rev. B **39**, 11406 (1989).

[10] S.L. Lee (private communication).
[11] S.L. Lee *et al.*, Phys. Rev. Lett. **71**, 3862 (1993).
[12] Y.Q. Song *et al.*, Phys. Rev. Lett. **70**, 3127 (1993); G. Blatter *et al.*, Rev. Mod. Phys. **66**, 1125 (1994).
[13] W.E. Lawrence and S. Doniach, in *Proceedings of LT 12, Kyoto, 1970*, edited by E. Kanda (Keigaku, Tokyo, 1971), p. 361.
[14] Same data as that used in Ref. 11. From S.L. Lee (private communication).
[15] M.V. Indenbom *et al.*, Physica C **222**, 203 (1994).
[16] P.G. de Gennes, *Superconductivity in Metals and Alloys* (Benjamin, New York, 1966).
[17] Since the magnitude of the effect in Eq. (9) does not depend on temperature for field-cooled BSCCO below about 75 K (Ref. 15), we took $\lambda_{ab} = \lambda_{ab}$ (75 K).